

DESIGN AND VALIDATION OF A REAL-TIME MODEL FOR STEADY-STATE AND TRANSIENT PERFORMANCE SIMULATION OF A HELICOPTER ENGINE

von Frowein J*, Abdullahi H*, Erhard W*, Schmidt K-J*

♦ FTI Engineering Network GmbH, Ludwig-Erhard-Ring 8, 15827 Blankenfelde-Mahlow, Germany

★ MTU Aero Engines GmbH, Dachauer Str. 665, 80995 München, Germany

* Technische Universität München, Boltzmannstr. 15, 85748 Garching, Germany

Abstract

The objective of this study was to establish a transient performance synthesis model of a helicopter engine which is fully functional in the whole operating range. A validated steady-state simulation model provided the basis for this work. To allow the simulation of the starting sequence, the original component characteristics first needed to be extended to the sub-idle region. With the aid of the theory of incompressible fluids, the maps of the compressor and turbine characteristics were extrapolated to zero speed. Moreover, the combustion model had to be improved taking fuel evaporation and chemical reaction effects into account. As a next step, the influence of diverse transient effects on the engine behaviour needed to be adapted in order to match a data set obtained during a test cycle in a test bed including the start sequence. Finally, a case study demonstrates the functionality of the engine model in combination with the control system. In this study, an emergency case is simulated where one of the helicopter's two engines fails and the remaining one quickly accelerates permitting safe landing. The simulated results of this case study as well as those of the adapted test cycle match their measured equivalents quite well.

Nomenclature

D	Sauter mean diameter
FRAC	primary combustion zone to burner volume ratio
I	starter electric current
N	rotational speed
P	total pressure
PW	shaft power
Q	heat transfer rate
Re	Reynolds number
t	time
T	total temperature
TRQ	shaft torque
U	starter voltage
v	velocity
V	volume
W	gas mass flow
WF	fuel flow

Δ	delta
η	efficiency
Θ	moment of inertia
λ	evaporation constant
π	Archimedes constant
Π	pressure ratio
Ω	air loading factor

Subscripts

0	ambient conditions
1	gas generator
2	power turbine / output shaft / rotor shaft
45	power turbine inlet plane
C	compressor
e	evaporation rate controlled
in	inlet value
is	isentropic
out	outlet value
r	reaction rate controlled
ref	reference
red	reduced
T	turbine

1. Introduction

The typical mission cycle of a helicopter turboshaft engine like the MTR390 consists of many accelerations and decelerations especially since it has mainly been developed for tactical aircraft. Therefore, transient effects caused by the inertia of the engine spools and the heat transfer between the working fluid and the engine components, for example, play an important role in the engine's service life and influence its performance considerably. A proper analysis of the engine behaviour needs to be based on a detailed transient simulation model of the engine. Such a model may help better understand the interaction between the engine and its control system. It can be used to examine any effects related to transient manoeuvres like the rotor droop or the power hole after an acceleration, for example, or the influence of the control laws such as different limiting turbine temperatures.

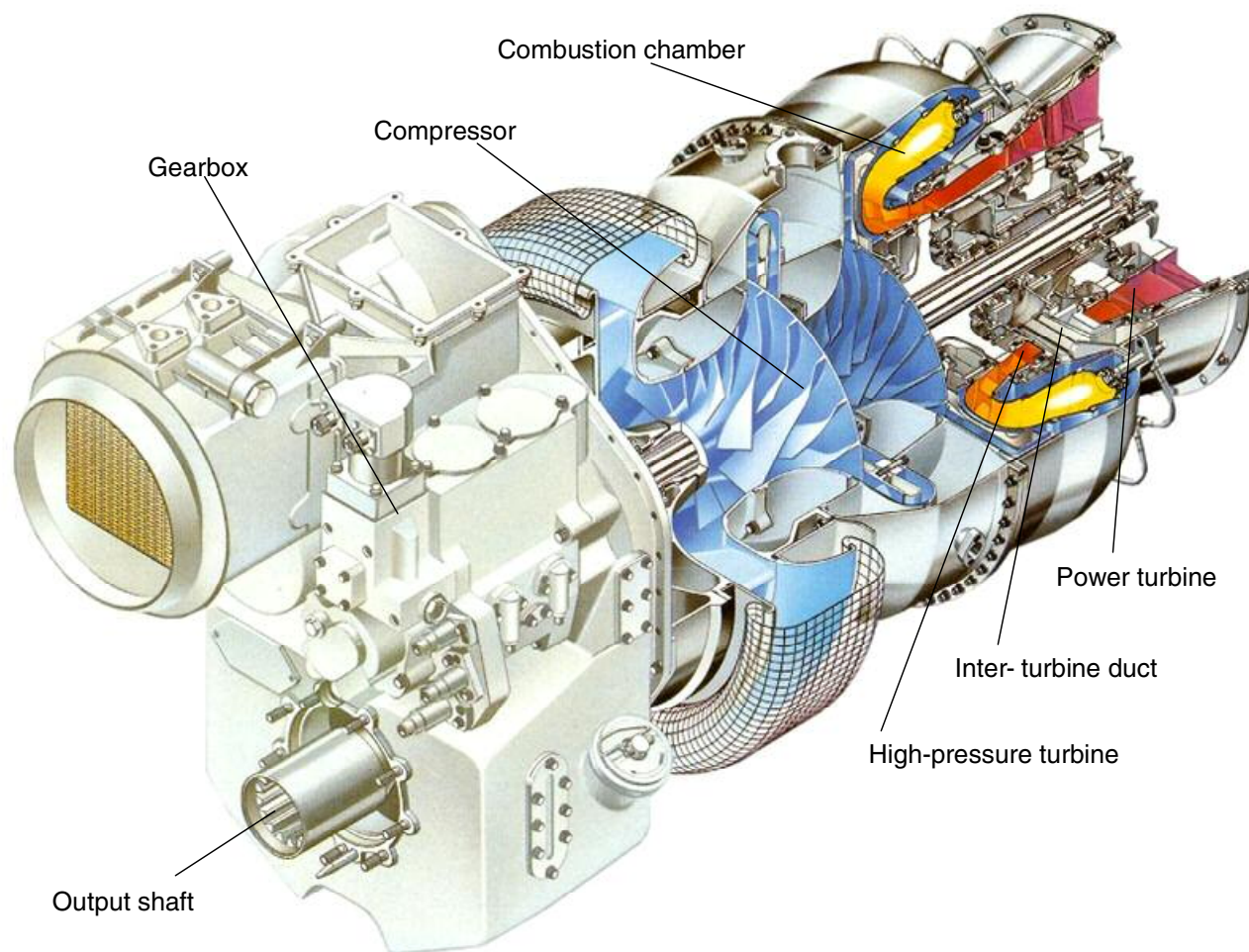


Fig. 1: MTR390 turboshaft helicopter engine

Also an analysis of the engine starting procedure is possible including ignition and extinction calculations. Another possible application of this kind of engine simulation model is the real-time testing of the functionality of control systems. In order to fulfil all these tasks an accurate performance simulation model of the engine and its control system is required which allows steady-state and transient calculations within the whole operating range including the sub-idle region. An already validated steady-state simulation model for operating points above idle provides the basis for this work. In a first step, this model has to be extended to the sub-idle region down to zero rotational speed. The maps of the compressor and two turbines are extrapolated on the basis of the theory of incompressible fluids. Moreover, the combustion chamber characteristics are improved, taking the fuel evaporation rate in addition to the chemical reaction rate into account. Subsequently, a transient calculation model can be superimposed, allowing the simulation of the desired transient effects. The resulting computer model is quite complex and the quality of its results depends on a great number of geometrical and physical parameters which characterize every engine.

These parameters need to be adapted so that the simulation results match the real-engine behaviour. A set of measured data which has been recorded during a pass-off test cycle of an MTR390 engine serves as the basis for the model adjustment and validation. The goal is to emulate the engine behaviour during this test cycle especially with regard to the acceleration and deceleration procedures and also the starting sequence. The functionality and application range of the engine model in combination with its control system is demonstrated in a case study. An emergency case, where one of the helicopter's two engines fails and the remaining one accelerates quickly in order to permit safe landing, is simulated and compared to measured values.

2. The engine and its control system

The studied object was an MTR390 turboshaft helicopter engine of the 1000 kW category which is jointly produced by the companies MTU, Turboméca and Rolls-Royce. Figure 1 shows the MTR390 engine ready for use in the helicopter. It consists of a two-stage centrifugal compressor, a reverse-flow annular combustion chamber, a

single-stage high-pressure turbine with an inter-turbine duct, a two-stage power turbine, a gearbox and a digital control and monitoring system. In operation each engine is controlled individually by a Full Authority Digital Engine Control system (FADEC), which means that the fuel flow is automatically calculated according to the pilot's commands, the environmental conditions and a set of measured engine parameters. The control system serves the purpose to reach a commanded output power safely and as quickly as possible in compliance with the engine limits.

The fast and precise gas generator control loop, limiting the spool speed N_1 as well as the spool acceleration \dot{N}_1 and the turbine temperature T_{45} , is overlaid by a power turbine control loop which is responsible for the restriction of the output torque as well as the output spool speed N_2 . This cascade control concept is advantageous because it separates the quickly responding gas generator from the power turbine and helicopter rotor with its limited dynamic behaviour resulting from the high moment of inertia. In order to minimize control deviations a priori, the system is supplemented by a feed-forward control, which calculates a preliminary gas generator spool speed demand according to the pilot's steering commands.

3. The functional engine model

The functional engine model, as shown in Fig. 2, consists of the transient performance synthesis model, the control system as well as models of the actuators and sensors. Control system, actuators and sensors are directly represented in Matlab/Simulink whereas the performance synthesis tool employed to simulate the engine behaviour, written in Fortran, is embedded as a S-function. The synthesis tool has a modular structure where the thermodynamic process of every engine component is represented by special sub-routines and the characteristics of each component are filed in special tabulated maps. The calculation is carried out in an iterative procedure employing the Newton-Raphson method until the results of the different modules converge to a final solution. Based on a steady-state simulation model of the engine, which already has been validated and adapted to an average production engine, a transient performance synthesis model is established.

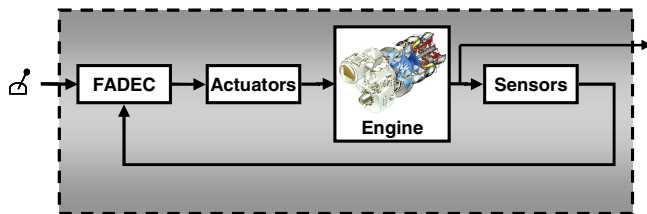


Fig. 2: Functional engine model including the transient model, the control system, the actuators and sensors

3.1 Simulation of transient phenomena

The transient calculation includes the physical effects of the moment of inertia as well as a complex heat transfer model. The moment of inertia affects the excess shaft power which is needed for acceleration, for example, according to this equation:

$$\Delta PW = 4 \cdot \pi^2 \cdot \Theta \cdot N \cdot \dot{N} \quad (1)$$

Thus, an acceleration of the gas generator spool from idle to take-off power can be achieved within few seconds and depends on the moment of inertia, the current spool speed and the surplus power provided by the high-pressure turbine. Within the heat transfer model every engine component is subdivided into few segments and each of these segments is considered to have a homogeneous temperature. Figure 3 illustrates for instance the heat transfer model of the high-pressure turbine.

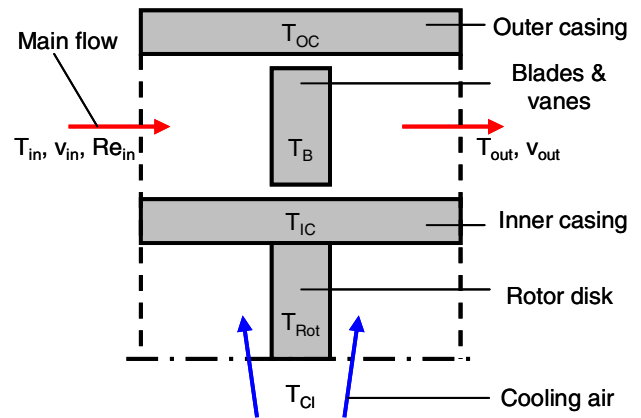


Fig. 3: Heat transfer model of a turbine

The turbine model consists of the segments 'outer casing', 'blades and vanes', 'inner casing' and 'rotor disk'. Inner casing and outer casing each are in convective contact with the gas flow whereas the rotor disk is in convective contact with the cooling air. Moreover, conductive heat transfer is allowed between inner casing and rotor disk. This interaction between the gas flow and the engine parts, known as heat soakage, results in a temperature change of the gas and thus in a gain or loss of specific enthalpy. Figure 4 shows the simulated heat transfer in the different engine components during an acceleration sequence from idle to take-off power. The highest peak of the heat transfer occurs in the combustion chamber, followed by the compressor, whereas especially the heat transfer in the power turbine dies out much more slowly than in the other components.

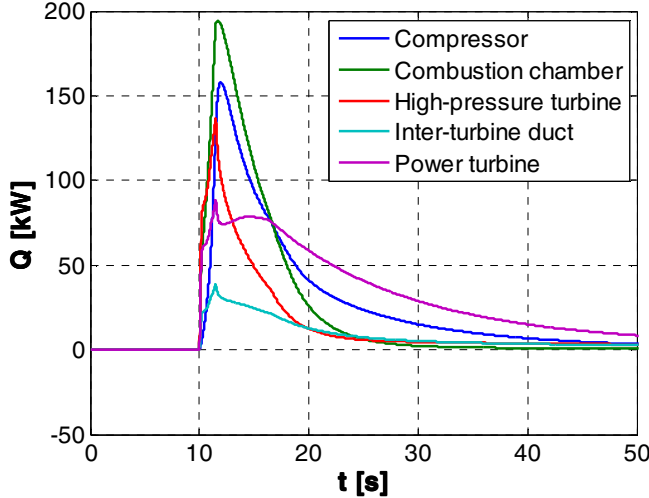


Fig. 4: Calculated heat transfer in the different engine components during an acceleration from idle to take-off power

Since, because of the heat soakage, neither the compression nor the relaxation of the gas can be considered an adiabatic process any longer, also the efficiency needs to be corrected. This efficiency change is calculated for compressors and turbines with equations (2) and (3) respectively.

$$\frac{\Delta\eta_{is,C}}{\eta_{is,C}} = \frac{\frac{T_{out}}{T_{in}} - 1}{\frac{T_{out}}{T_{in}} - 1 - \frac{1}{2} \frac{\Delta T_{out}}{T_{in}} \ln \frac{T_{out}}{T_{in}}} \quad (2)$$

$$\frac{\Delta\eta_{is,T}}{\eta_{is,T}} = \frac{\ln \frac{T_{out}}{T_{in}}}{2 \left(\frac{T_{out}}{T_{in}} - 1 \right) T_{in}} \Delta T_{out} \quad (3)$$

ΔT is the temperature difference between the actual transient state and the steady state. The deduction of these formulas can be found in [1]. The changing temperature of the engine parts also causes an expansion or contraction of the structure. Due to its thermal inertia the rotor disk expands considerably slower than the outer casing, which results in a variation of the tip clearance between the rotor blades and the outer casing. This again leads to a change of efficiency of the turbo components. The tip clearance is calculated with a linear expansion model of the different component segments and the change in efficiency caused by a certain clearance has been closely examined during a rig-test on the results of which the simulation is based. For the transient simulation under extreme part-load conditions, it is important to change the original map-based values of the efficiency not by adders but by scalars since adding negative values to a very small efficiency may wrongly result in

negative efficiencies, for example, and therefore cause numeric problems. The time span during which the heat transfer and the effects derived from it influence the performance of the engine after a considerable change of the operation point can take up to 300 seconds.

The transient simulation model obtained is based on a great number of parameters whose accuracy is an important factor for the quality of the simulation results. On the one hand, these parameters consist of geometrical values and reduced Nusselt numbers which are calculated on the basis of engineering detail drawings. On the other hand, the parameters specify material properties which are averaged over the operating temperature range. As these original parameters have been calculated assuming simplified geometrical models of the engine parts, these values still need to be slightly adjusted on the basis of the comparison of the simulation results with measured data.

3.2 Extrapolation of the turbo component maps

As mentioned before the characteristics of each turbo component are filed in different tabulated maps which are based on the Mach number similarity. The commonly used parameters are the reduced speed, the reduced mass flow, the efficiency and either the pressure ratio or the reduced specific work. In order to allow simulations of starting or in-flight restarting procedures, the engine behaviour in the sub-idle region must also be taken into account. This region, however, is normally not examined during standard rig tests simply because the instrumentation is usually designed for tests distinctly above idle [2]. Thus reliable measurements below this range are quite rare and an extrapolation of the maps needs to be based on theory rather than on experimental results. The theory of incompressible fluids and the representation using different combinations of the work, pressure and flow coefficient is well suited for this task because for low gas speeds the influence of the Mach number diminishes for these parameters. A detailed description of the extrapolation method used and the underlying theory can be found in [3].

After the extrapolation, the regular parameters reduced speed, reduced flow and pressure ratio/specific work still remain valid for the map representation. Only the efficiency definition causes problems if the pressure ratio drops to values close to one. For a compressor, the efficiency changes from $-\infty$ to $+\infty$ if the effective specific work drops below zero and the same problem occurs concerning the turbine efficiency if the isentropic specific work passes through zero. These singularities may keep the iterative synthesis calculation from converging and should therefore be avoided. This can be achieved by replacing the efficiency by the reduced torque parameter $TRQ_{red} = TRQ / (W\sqrt{T})$ which remains continuous over the whole operating range and even allows calculations at zero speed [3].

Figure 5 shows the extrapolated compressor map with the reduced torque contours and a steady-state working line at ISA sea level static conditions. The image also shows a comparatively wide flow range at low speeds, which is typical for centrifugal compressors and which is also the reason why bleed valves are not needed for stable operation in this range.

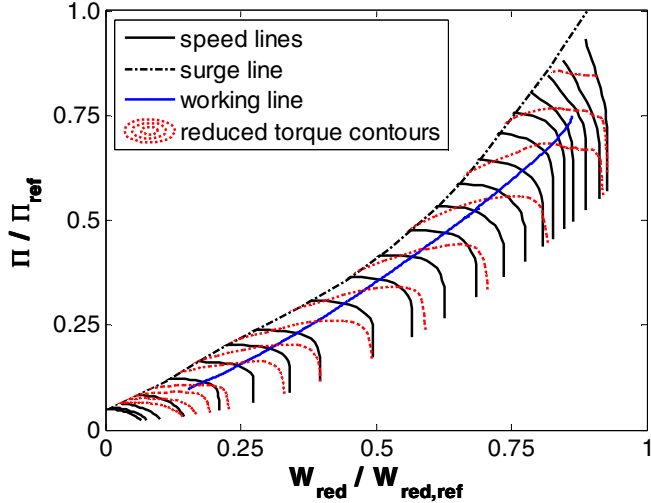


Fig. 5: Extrapolated compressor map with reduced torque contours

3.3 The combustion chamber characteristics

According to [4] in general the combustion efficiency is mainly limited by the fuel evaporation rate or the chemical reaction rate of the fuel-air mixture. In the operating range above idle the reaction rate usually plays a major role and the evaporation rate can be neglected. This combustion model, as it is described in [5], has already been used for the original steady-state simulation and derives the combustion efficiency η_r from the air loading factor Ω .

$$\Omega = \frac{W}{P^{1.8} \cdot V \cdot 10^{0.00145 \cdot (T-400)}} \quad (4)$$

$$\eta_r = f(\Omega) \quad (5)$$

But experimental results show that at slow gas speeds in the sub-idle region the burner efficiency decreases even though the air loading factor is very low due to the small air flow and therefore the efficiency should be very high. This indicates that close to zero speed another model is required. In this case, the evaporation process appears to be the decisive factor of the efficiency determination. Reference [4] proposes the following formula for the calculation of the evaporation-controlled efficiency:

$$\eta_e = 1 - \exp\left(\frac{-36 \cdot 10^6 \cdot P \cdot V \cdot \lambda_{fuel}}{FRAC \cdot T_{ideal} \cdot D^2 \cdot W}\right) \quad (6)$$

The evaporation-controlled burner efficiency depends on the evaporation constant λ_{fuel} , the Sauter mean diameter D and the ideal combustion temperature T_{ideal} in addition to the factors already included in the reaction-rate controlled efficiency calculation. The overall burner efficiency is obtained by multiplying η_r and η_e . If the air mass flow W drops now towards zero the overall efficiency decreases, as well.

4. Engine model adaptations

4.1 Adaptation approach

The pass-off data which the simulation is supposed to match was obtained during a test cycle on an engine test bench that included several accelerations and decelerations between idle and take-off power at a sensing frequency of 20 Hz. The data set consists basically of the following values:

T_0	Ambient temperature
P_0	Ambient pressure
N_1	Gas generator spool speed
N_2	Power turbine /Output shaft speed
T_{45}	Power turbine inlet temperature
WF	Fuel flow
TRQ	Output shaft torque
I	Starter electric current
U	Starter voltage

To compare the synthesis engine model with the measured data the sequences of fuel flow, torque and the ambient conditions are used as input for the open-loop engine model. During an open-loop simulation process the deactivated control system cannot affect the calculated engine behaviour with its correcting influence. The performance synthesis tool can thus calculate the transient engine behaviour according to the input sequences and output any thermodynamic value, the mass flows, spool speeds and the resulting output power. Subsequently the results of the spool speeds N_1 and N_2 as well as the temperature T_{45} can be compared to the measured values, as shown in Fig. 6 and 7.

The measured results of the power turbine inlet temperature T_{45} contain a certain latency in reference to the actual gas temperature. This latency needs to be taken into account when measured and simulated results are compared. The thermal inertia of the probe is emulated by a second-degree dynamic model. A time constant represents the delay caused by the heat conduction inside the measuring probe and a second term, depending on the spool speed and there-

fore on the gas velocity, stands for the time needed for the convective heat transfer from the gas to the probe.

As Fig. 6 demonstrates, the simulation results based on the initial parameter values differ considerably from the measured values especially with respect to the power turbine spool speed. This divergence does not only appear during the transient phases of the test cycle but also during steady-state operating modes. The fact that the original steady-state model has only been calibrated for gas generator spool speeds $N_1 > 78\%$ explains the large divergences below this value. Therefore, the simulation model needs to be adapted regarding the steady-state and the transient engine behaviour.

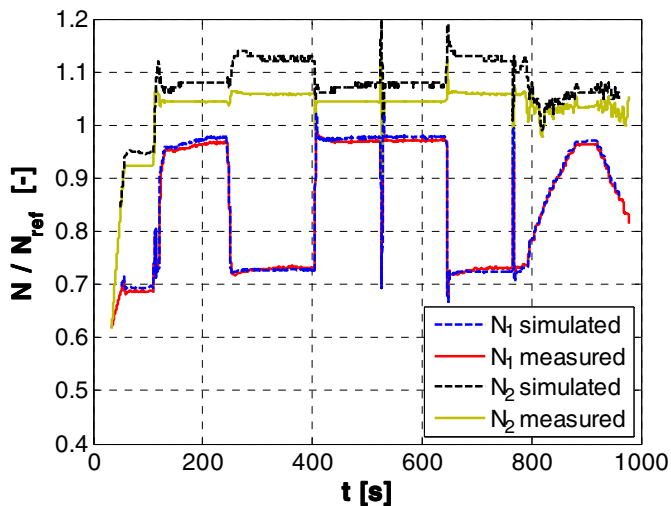


Fig. 6: Comparison of the measured and simulated values of the spool speeds N_1 and N_2

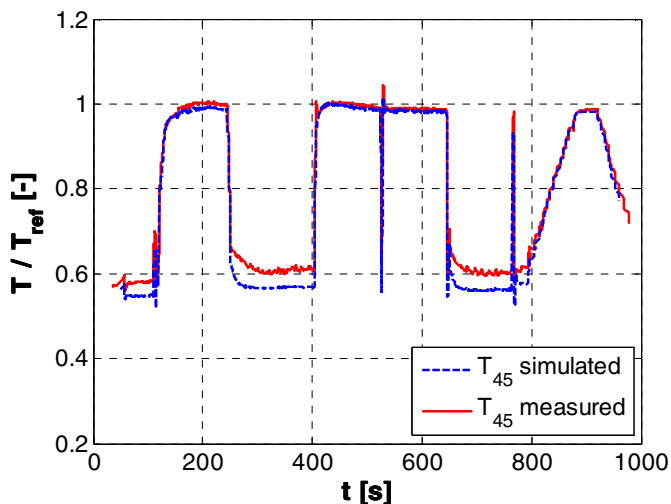


Fig. 7: Comparison of the measured and simulated values of the power turbine inlet temperature T_{45}

4.2 Model adaptation

The reason why the results differ in a steady-state operating mode, in spite of the previous stationary model calibration, is the production scatter of the engine parts. And due to the production scatter the component characteristics may vary a little from engine to engine. This kind of distribution can be observed for a variety of engine parameters. Added up, all these small variations can influence the engine steady-state behaviour to some extent. The goal, however, is not the match of an average engine but of a specific engine and therefore at first a steady-state model adjustment has to be carried out. The distributions of these parameters in the series engines have already been examined in previous studies. And therefore the ranges in which the variations of the model parameters have to remain are well known. An effect study is carried out to analyse the influence of every possible parameter variation within the simulation. With the help of this effect study and taking the limited distribution range of the varying parameters into account, the steady-state adaptation can be accomplished.

The transient adaptation is carried out in a similar way. At first the impact of every transient effect in each engine component is quantified. For this purpose two runs of the test cycle are needed for each transient effect. During the first simulation run the examined effect needs to be turned off, whereas the second run is conducted as usual with every effect switched on. Subsequently, the data of those two runs can be compared and the difference of the values achieved in the two cycles provides information in how far the examined effect influences the engine behaviour. Now the deviations of the simulation results can be compared to the characteristics of the different transient effects in terms of their characteristic time profile and their magnitude, which then allows a model adaptation. Since in some cases it is difficult to identify whether a certain parameter change has a positive effect over the whole sequence or not, an error value is calculated for each simulation run which determines the average error. So an objective comparison of every change is possible. The results of the complete adaptation are shown in Fig. 8 and 9.

The results of the transient adaptation correspond well with their measured equivalents regarding the profile of the spool speeds as well as the profile of the temperature. It can be observed, however, that an exact adaptation of the heat transfer is only possible for either accelerations or decelerations. In order to be able to simulate both manoeuvres a compromise has been made which yields good results for all kinds of accelerations, but only for comparatively slow decelerations. At a rapid deceleration the spool speed N_2 overshoots, as it is shown in Fig. 8 at $t=650s$. The heat transfer appears to be too strong. A possible explanation is the fact that heat flows and energy losses from certain component parts are neglected and therefore the stored energy

from a higher operating point is completely returned to the main gas flow after a deceleration. Therefore, too much energy is available in the gas flow which can be converted into output power. Another possible way to improve the simulation is the calculation of the component material parameters as a function of the component temperature. So far, the simulation only allows averaged values of these parameters, which are used for the determination of the heat transfer coefficient or the thermal expansion of the engine parts, for example. In most cases, however, the behaviour during accelerations is more critical than that during very fast decelerations and there the simulation provides reliable results.

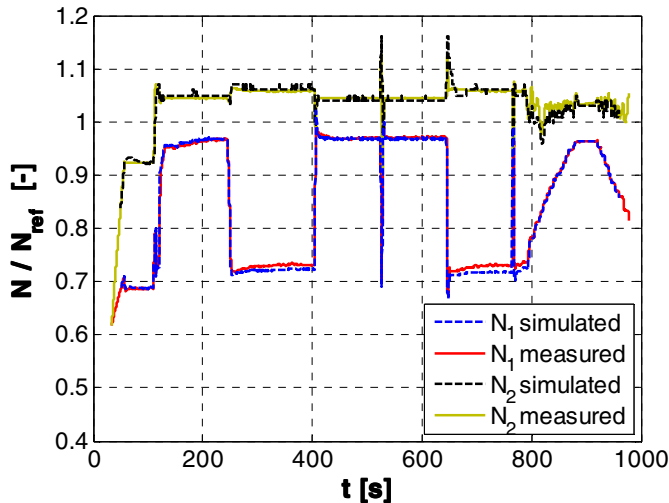


Fig. 8: Comparison of the measured and simulated values of the spool speeds N_1 and N_2

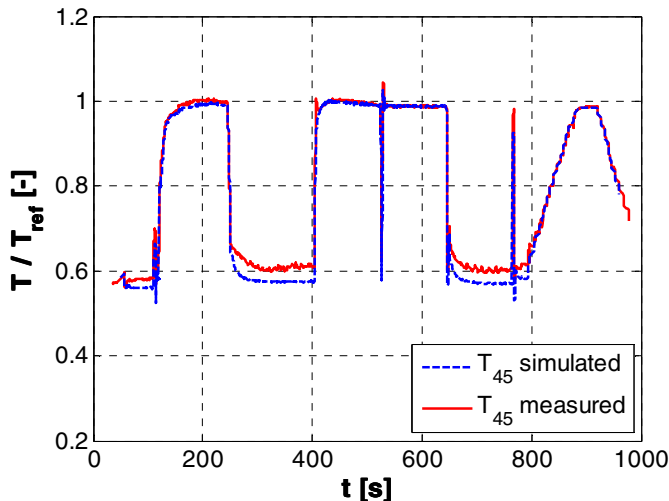


Fig. 9: Comparison of the measured and simulated values of the power turbine inlet temperature T_{45}

4.3 Engine starting sequence

As a next step the starting sequence is examined. The automatic starting sequence is usually processed as follows: at first the electric starter helps accelerate the gas generator spool for about 20 seconds. During this period the combustion chamber is ignited as soon as stable ignition conditions can be assured. A self-contained operating mode of the engine without starter is possible only above a spool speed N_1 of about 30%. The spool is accelerated up to a ground idle speed of about $N_1=68\%$ and the power turbine spool follows with a certain time lag and stabilizes at about $N_2=92\%$. Above ground idle, N_2 is regulated to a nearly constant value of about 104%.

The simulation of a starting process can help investigate the required starter torque or the time needed to start the engine under varying environmental conditions. It can also provide information about the ability of the engine control to execute and monitor a successful engine start. The adaptation of the starting procedure was particularly complicated because no stationary comparative values are available, since during a normal starting process, the range up to ground idle is passed through as a part of a rather quick acceleration. This means that it is hardly possible to separate the transient effects from the engine steady-state behaviour regarding the measured values. In addition, the instrumentation is not mainly designed for this operating range and thus the measured results, especially the temperature values, are not as reliable as at higher speeds.

The simulation is based on the extended combustion model and the extrapolated component maps. The starter power is a result of the input voltage, the electric current and the estimated starter efficiency. The simulation results are shown in Fig. 10 and 11 and compared to measured values. The corresponding sequence up to take-off power is also traced in the compressor map, as shown in Fig. 12. This illustration confirms that the engine operates without bleed even during the start phase, as the two-stage compressor has sufficient surge margin.

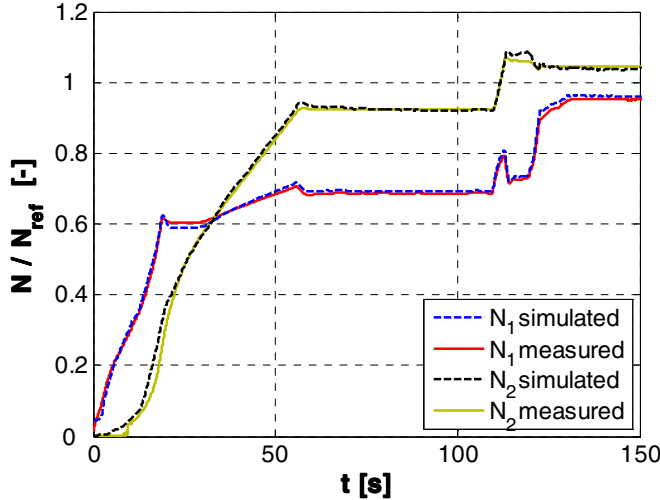


Fig. 10: Comparison of the measured and simulated values of the spool speeds N_1 and N_2

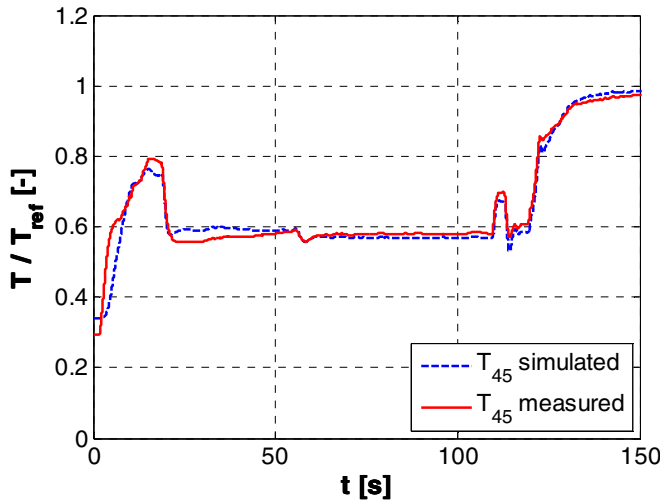


Fig. 11: Comparison of the measured and simulated values of the power turbine inlet temperature T_{45}

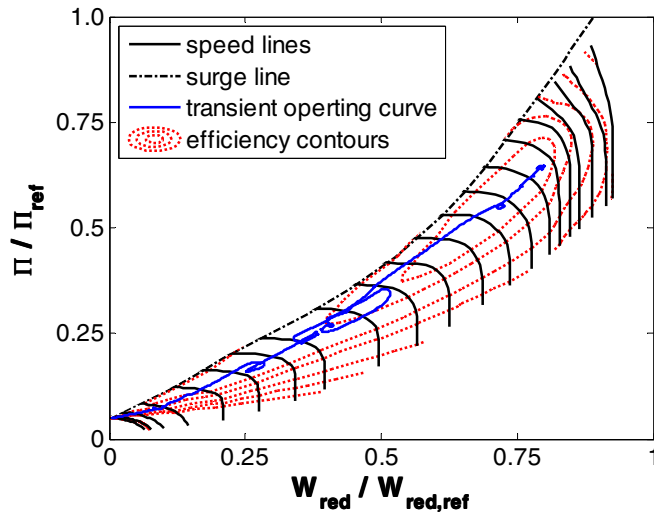


Fig. 12: Transient operating curve in the compressor map

5. Case study

So far the simulation has been adjusted for one specific engine which was run in a test stand. Now the question arises how closely the simulation matches the behaviour of a different production engine in a flight manoeuvre. For this purpose, a failure of one of the two helicopter engines is simulated at a hovering altitude of about 5 meters. Under these conditions the remaining engine has to accelerate quickly to ensure a secure landing procedure which should be as smooth as possible. The simulated results can be compared to measured equivalents.

If one of the two helicopter engines breaks down during flight the remaining engine has to guarantee a safe landing procedure. If this scenario occurs few meters above the ground a quick acceleration of the operative engine is particularly important. Since an immediate compensation of the lost power is not possible the helicopter will not be able to stay at its altitude. In order to slow down the helicopter the pilot normally applies the collective pitch and increases the angle of attack of the main rotor blades shortly before touch-down. By doing so the kinetic energy of the main rotor can be converted into lift and the vertical velocity decreases.

For an adequate processing of the input commands the rotor characteristics have been integrated into the computer model. Instead of demanding a certain load or a rotational speed the user can now demand a certain angle of attack of the rotor blades and within the model the required torque of the main and tail rotors is determined as a function of the rotational speed N_2 and the angle of attack. Torque and moment of inertia of the rotors are divided by the number of operative engines, which permits the simulation of an engine break-down.

The following simulation is started at a hovering altitude of about 5 meters where one engine fails after 6 seconds. The overall output power drops considerably because the remaining engine cannot immediately provide the demanded power, see Fig. 13. Therefore, also the rotational speed N_2 decreases. The remaining engine accelerates automatically. After another three seconds, the pilot increases the angle of attack of the main rotor blades, which causes a further drop of the rotor speed but increases the lift for a short period of time and thus decreases the vertical landing speed. After touch-down at about $t=10s$, the demanded angle of attack can be reduced and the power output decreases whereas the rotor can recover its speed, see Fig. 14.

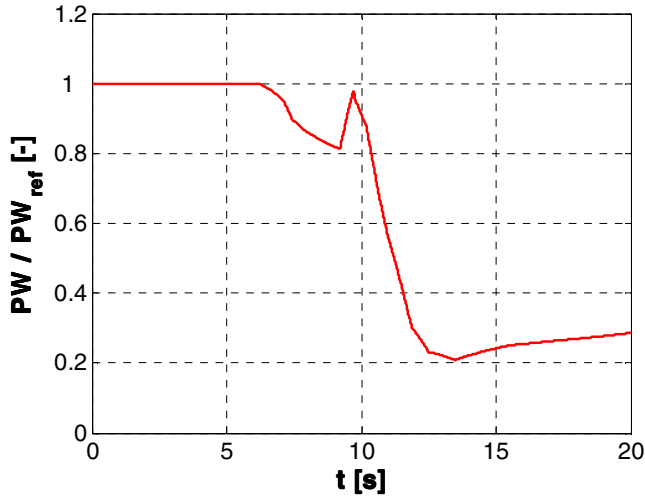


Fig. 13: Development of the rotor shaft power taking the number of working engines and the rotor inertia into account

As mentioned before the steady-state behaviour differs a little from engine to engine. Hence, for every specific engine, the steady-state model needs to be adjusted according to its production scatter variations. The influence of the transient effects, however, should remain at a comparatively constant level. On the one hand, the impact of this landing strategy can be reconstructed and on the other hand the engine behaviour is analyzed and compared to the corresponding measured data which were obtained during an in-flight experiment. As Fig. 14, 15 and 16 demonstrate, the simulated behaviour is quite well in line with the test data.

6. Concluding remarks

Transient performance synthesis models are inevitable in the design, development and in-service phases of an engine. In this study an engine model has been presented which is capable of simulating the whole operating range including the sub-idle region. Comparisons show that the model is quite well in line with the test data gained from a production engine with limited test parameters. The first trials of a modified model where input from and output to a computer hard disk are unnecessary, showed also very promising real-time capabilities. For further improvements of the model, the next steps of the research will consider the temperature dependency of the material properties of the engine components. A validation of the model will be carried out using more exact test data, especially of the component material temperatures obtained using an extensive measurement instrumentation.

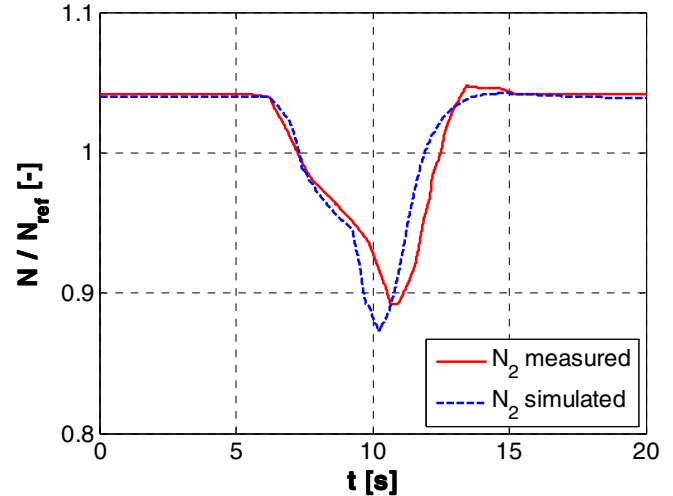


Fig. 14: Comparison of the measured and simulated values of the main rotor speed N_2

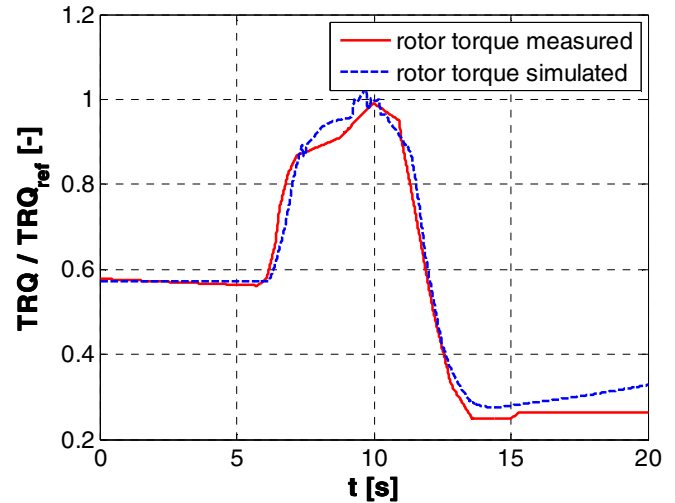


Fig. 15: Comparison of the measured and simulated values of the shaft torque TRQ

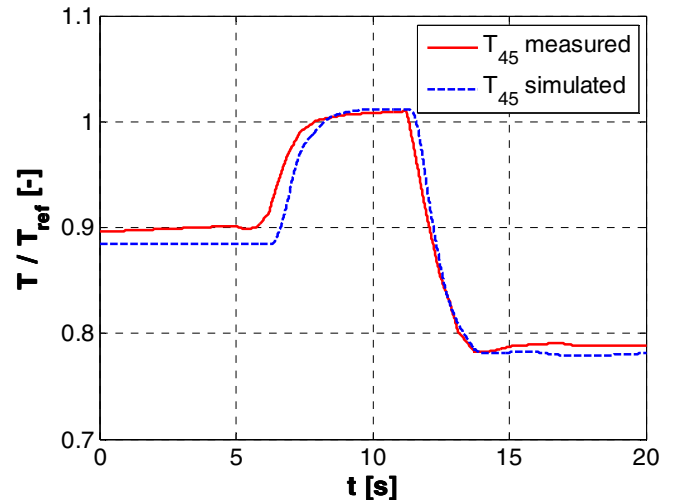


Fig. 16: Comparison of the measured and simulated values of the power turbine inlet temperature T_{45}

Acknowledgements

This paper is based on a thesis research work that was sponsored by MTU Aero Engines. The authors owe Klaus Lietzau a debt of gratitude for his assistance concerning the simulation of the control system and Werner Popp at Eurocopter for the feedback about the in-flight engine behaviour. Further the authors wish to thank their colleagues who were always available for discussions about this work and MTU Aero Engines for the permission to publish this paper.

References

- [1] Bauerfeind K.
Die Berechnung des Übertragungsverhaltens von Turbostrahltriebwerken unter Berücksichtigung des instationären Verhaltens der Komponenten, Luftfahrttechnik- Raumfahrttechnik, Heft 5/6/1968, VDI Verlag, Düsseldorf
- [2] Bauerfeind K.
Steuerung und Regelung der Turboflugtriebwerke, Birkhäuser Verlag, Basel, 1999
- [3] Riegler C., Bauer M., Kurzke J.
Some Aspects of Modelling Compressor Behavior in Gas Turbine Calculations, 2000-GT-574, ASME Turboexpo, Munich, 2000
- [4] Lefebvre A. H.
Fuel Effects on Gas Turbine Combustion, 16th CIMAC Congress, Oslo, 1985
- [5] Walsh P. P., Fletcher P.
Gas Turbine Performance, Blackwell Science, Oxford, 1998